Mon. Not. R. Astron. Soc. **000**, 000–000 (0000) Printed 1 February 2008 (MN LaTeX style file v1.4)

The luminosity dependence of opening angle in unified models of active galaxies.

C.M. Rudge and D.J. Raine
Astronomy Group, University of Leicester, University Road, Leicester, LE1 7RH, UK.

1 February 2008

ABSTRACT
In unified models of active galaxies the direct line of sight to the nucleus is unobscured only within a certain cone of directions. An opening angle for this cone is usually estimated by methods such as the overall ratio of Seyfert 1s to Seyfert2s, the latter assumed to be obscured versions of the former. Here we shall show, as has often been suspected, that the opening angle of the cone depends on the luminosity of the central source, with higher luminosities corresponding to larger opening angles. This conclusion depends only on the assumption that the width of the broad emission lines at a given luminosity is a measure of inclination angle, an assumption that is supported by observation in radio-loud systems. On the other hand we show that the scatter in X-ray spectral index is not primarily an effect of viewing angle, in contrast to what might be expected if the scatter on the spectral index versus luminosity relation were a consequence of absorption in the obscuring material. The observed correlation between linewidth and spectral index appears to be a further consequence of the dependence of opening angle on luminosity.

Key words: galaxies: active: – galaxies: Seyfert – quasars: emission lines

1 INTRODUCTION

The basic structure of an active galactic nucleus (AGN) includes a central continuum source and emission line gas, which, for some lines of sight is blocked from direct view by obscuring material of some form, possibly having the geometry of a torus. Viewed along the opening cone of the torus such systems appear as unobscured Seyfert 1 nuclei (in the radio-quiet case), while from greater inclinations to the axis of the torus the broad lines cease to be directly visible and they appear as Seyfert 2s. These are analogous to type 1 and 2 QSOs in the radio-loud case. It has been clear from the outset that this simple picture, in which the opening angle of the torus is fixed for all systems, is unlikely to be true (Antonucci 1993). In this paper we shall show that the available data on the linewidth distribution of the broad emission lines can be interpreted in terms of an opening angle that increases with luminosity.

The conclusion depends on the assumption that we can use the broad line widths at given luminosity to measure the angle of inclination of the axis of the obscuring matter to the line of sight. This implies both that the broad line region (BLR) is axisymmetric and that its axis coincides with that of the obscuring material. In the case of radio-loud systems the axis of radio emission can be shown to correlate with broad line widths (Wills & Browne 1986) implying that the BLR is axisymmetric and aligned orthogonally to the radio axis. In radio-quiet systems we have shown (Rudge & Raine 1998) that the distribution of scatter on the linewidth – luminosity relation can be accounted for in terms of inclination. We examine these points further in section 2.

At first sight we should be able to use our relation between linewidth, luminosity and inclination angle to measure the inclination of individual systems. Despite the agreement with the statistical distribution however, we appear to find problems carrying this out, specifically that for a number of galaxies there is no solution for the angle. The reason for this can be readily seen if we bin the data into luminosity ranges and allow the distribution in $\sin i$ of the objects to be determined by the data. We find that i is restricted to a range $i < i_*$ where i_* increases with luminosity L (section 5). We take i_* as a measure of the opening angle in the unified model. Our original assumption that systems have random inclination, i.e. $\sin i$ is uniformly distributed in $[0, \pi/2]$, is therefore not valid. We expect that the distribution of $\sin i$ is constant at each luminosity, but the limited size of the data set does not show this clearly.

In section 6 we consider the proposed anti-correlation between broad line widths and the X-ray spectral index, $\alpha_{\rm x}$ (Borson & Green 1992; Wandel & Boller 1998; Puchnarewicz et al. 1997). We show that this is not primarily driven by a dependence of $\alpha_{\rm X}$ upon viewing angle, as might be expected from the dependence of FWHM upon orientation.

The observed anti-correlation is at least partially due to the increased range of viewing angles at higher luminosities.

2 EVIDENCE FOR AXISYMMETRY IN THE BROAD LINE REGION

The radio power in radio galaxies is generally accepted to be an indicator of viewing angle to the central source, with the flat spectrum core dominant in face-on systems and the steep spectrum lobes dominant in edge-on systems. The ratio of core to lobe radio power, R, correlates with the width (FWHM) of Hβ in the sense that the broadest lines are seen in more edge-on systems (Wills & Browne 1986). Wills & Brotherton (1995) develop this further with the introduction of a new parameter, R_ν. This is defined to be the ratio of radio core luminosity at 5GHz rest frequency to the optical V-band luminosity - improving the measure of orientation. They show that R_ν has a stronger correlation than R to the jet angle in a sample of 33 FR II sources. Further they show that using R_ν rather than R also improves the correlation with $\mathrm{FWHM}_{\mathrm{H}\beta}$ for both the Wills & Browne (1986) objects and a new sample of low-z quasars (Brotherton 1996), thus strengthening the case for an axisymmetric BLR in radio-loud systems. This evidence is supported by the correlation between FWHM and α_{ox}. The optical continuum is boosted by the jet in the face-on systems giving a viewing angle dependence for the optical to X-ray spectrum slope α_{ox}.

The case is much less clear for the radio-quiet systems. Here we have no such obvious inclination indicators as the jet angle. However, there is little, if any, strong evidence to suggest that the BLR in radio-quiet systems should be significantly different to that in the radio-louds. Studies of the distribution of line widths for radio-quiets and louds show only a small difference in the distributions with the radio-louds having generally wider lines (Corbin 1997). However, the radio-loud systems in this sample have a higher average luminosity. Since higher luminosity systems have on average broader lines, at least for CIV and Hβ, the result is what we would expect if the systems are drawn from a common population. Marziani et al. (Marziani et al. 1996) consider in more detail the differences between the profiles of Hβ and CIV lines in radio-loud and radio-quiet systems. They conclude that the line profile properties indicate that the BLR in radio-louds is not the same as that in radio-quiets. We shall discuss their findings in the context of the results of this paper in section 7. Boroson (1992) argues against a viewing angle dependent picture of radio-quiet AGN in which *both* the continuum and line emission are axisymmetric by consideration of the lack of correlation between the equivalent width of [OIII] and the FWHM of Hβ. The sample is selected by UV excess which may produce a bias against edge-on objects. In addition, according to the picture to be developed here, the range of angles for a low luminosity radio-quiet sample may be rather small, so the evidence may not be conclusive. In any case, all we require here is that the broad line region kinematics be axisymmetric, not that the illuminating continuum should be too.

From a theoretical point of view spherical BLRs dominate the literature. However, to provide the observed variations in profile shape with width (Stirpe 1991) such systems have to be quite complex. For example Robinson (1995) uses a changing radial depth and radial power laws for the velocity and emissivity of the gas to obtain the range of profile shapes. Nevertheless, while this provides an adequate account of individual systems, it is not clear whether models of this type can fit the linewidth distribution. A number of simple flow geometries in spherical systems are ruled out by detailed observation. For example, for NGC 3516, Goad et al. (1999) exclude both radial flows at constant velocity and Keplerian motion. Spherically symmetric systems also do not appear to be able to account for the change in profile shape with line width or the range of widths at each luminosity needed to be able to account for the distribution of linewidths (Rudge & Raine 1998). Simple disc geometries are also ruled out by consideration of the change in profile shape with linewidth (Stirpe 1991). However more complex systems such as the dual winds model of Cassidy & Raine (1996) or the VBLR–ILR model of Wills et al. (1993) adopted by Puchnarewicz et al. (1997) are able to predict the change in profile shape with linewidth required by observation (Stirpe 1991).

An alternative approach (Gaskell 1982; Dumont & Colin–Souffrin 1990) envisages a two-zone model which distinguished between high and low ionization lines. Originally prompted by the systematic blueshift of CIV relative to the Balmer lines, which suggested origins in regions of different kinematics, and by considerations of energy balance, the idea has received some support from reverberation mapping. The Hα transfer function peaks away from zero delay (for example in NGC 3516, Wanders& Horne 1994), consistent with a flattened cloud distribution, while the CIV response is immediate (for example NGC 5548, Korista et al. 1995), implying material in the line of sight. As a result the high ionization region (HIL) is often taken to be spherical, although alternative geometries are also consistent with echo mapping (Marziani et al. 1996). Although elsewhere we have argued that the statistical properties of the Hβ, MgII and CIV linewidth distributions do not indicate substantial differences between HIL and LIL geometries, the arguments in this paper depend only on the validity of some orientation effect in both Hβ and MgII. While MgII emission is often taken to be associated with the Balmer lines, and certainly arises from a region more extended than that producing CIV (from observed cross-correlation functions), it should perhaps be born in mind that we lack independent evidence for the geometry of the MgII emitting region.

The current work therefore provides a further self-consistency argument for axisymmetry in the BLR.

3 LINE WIDTH DISTRIBUTION

One of the reasons for developing a viewing angle dependent model is the need for some parameter, other than luminosity, upon which the FWHM of the broad emission lines depends. It is of course possible that the dominant parameter could be something other than viewing angle. Perhaps the most obvious choice would be black hole mass, M. However the success of a model (Rudge & Raine 1998) in which the unknown parameter varies as a sine function suggests that this is not the case: it is surely unrealistic to suggest that M has only part of a sine distribution. Furthermore, we will show in this paper that the range of values taken by this parame-

ter increases with luminosity. Assuming that $L \propto M\dot{M}$ then we would expect M to take a smaller, rather than larger, range of values at higher luminosities.

Thus we assume that, in general, the FWHM, v, of a given broad emission line in an axisymmetric system can be given as a function of the ionising luminosity and the inclination of the system. This function can be expanded in spherical harmonics with luminosity dependent coefficients. In a previous paper (Rudge & Raine 1998) we showed that the distribution of linewidths could be reproduced if this function were taken to be axisymmetric and only the first two terms of this series were retained, with the coefficients taken to have a common dependence on luminosity. The FWHM of a given emission line is then given by

$$v = (a + b \sin i) L^{\alpha} \tag{1}$$

with the constants a, b and α being chosen for each emission line. The inclination angle, i, is the angle of the line of sight to the axis of the BLR i.e. $i = 0$ for face-on systems. In Rudge & Raine (1998) we took L to be the B-band luminosity.

Since it is difficult to determine the line of sight angle for individual systems, at least with any accuracy, we are led to consider the linewidth distribution rather than the linewidths of individual objects. Assuming that the inclination of AGN is random across the sky, then the number of systems at each v is given by

$$N(v) = \int \frac{\sin i}{\left|\frac{\mathrm{d}v}{\mathrm{d}i}\right|} \Phi(L) \mathrm{d}L \tag{2}$$

where $\Phi(L)$ is the luminosity function giving the distribution of luminosities. In Rudge & Raine (1998) we used the luminosity function of Boyle, Shanks & Peterson (1988). In the later work on cosmology (Rudge & Raine 1999) we used the X-ray luminosity function of Boyle et al. (1994) and also the optical luminosity function of Pei (1995). In this paper, for convenience, we will again use the X-ray luminosities. Boyle et al. (1993) show that $L_{\mathrm{x}} \propto L_{\mathrm{opt}}^{0.88\pm0.08}$ and thus using X-ray rather than optical luminosities will only result in the requirement of a different value of α in (1).

Having developed this model and shown its success in accounting for the linewidth distribution (Rudge & Raine 1998) we now use it to consider the viewing angle of individual systems. For this purpose we again use data from the RIXOS sample (Puchnarewicz et al. 1996; Puchnarewicz et al. 1997). This provides comprehensive data on X-ray and optical continuum luminosities as well as spectral indices, line strengths, equivalent widths and FWHM. Rearranging (1) gives

$$\sin i = \frac{1}{b}\left(\frac{v}{L_{44}^{\alpha}} - a\right). \tag{3}$$

where L_{44} is the ROSAT 0.5–2 KeV luminosity in units of $10^{44}\,\mathrm{erg\,s^{-1}}$.

The method for finding the orientation for each system relies on finding a good fit to the linewidth distribution for a sample of objects and then using the values of a, b and α in (3). It is therefore important that the distribution is accurately modelled. We found that it is no longer sufficient to assume that the given sample has a luminosity distribution which matches the global luminosity function, or that the distribution of $\sin i$ is uniform - i.e. systems are at random

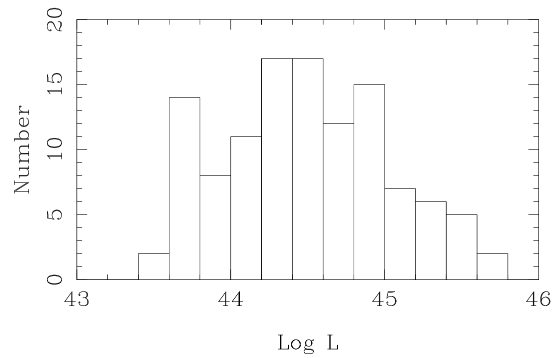

Figure 1. Luminosity distribution of the objects in the sample with measured $\mathrm{FWHM_{MgII}}$. L is the total ROSAT 0.5–2keV band luminosity.

orientation. In such a situation we found that, although the linewidth distribution could be matched, it was not possible to generate simultaneously values of $\sin i$ all lying in the range 0 to 1.

We therefore have to adopt an iterative procedure. In place of $\Phi(L)$ in (2) we use the actual number of systems in each luminosity bin, $S(L)$, for the selected sample. Similarly we need to replace $\sin i/|\mathrm{d}v/\mathrm{d}i|$ with $T(\sin i)/|\mathrm{d}v/\mathrm{d}\sin i|$ where $T(\sin i)$, the number distribution of $\sin i$, is calculated by consideration of the whole sample in (3). We shall find that the $\sin i$ distribution is also luminosity dependent and so we will in fact use $T(\sin i, L)$, which, in practice, is determined for a set of discrete luminosity ranges. Clearly we have to iterate to find $T(\sin i, L)$ and $N(v)$, by choice of a, b and α in (1), simultaneously in the revised linewidth distribution

$$N(v) = \int \left|\frac{\mathrm{d}\sin i}{\mathrm{d}v}\right| T(\sin i, L) S(L) \mathrm{d}L. \tag{4}$$

4 DATA FROM THE RIXOS SAMPLE

The ROSAT International X-ray/Optical Survey (RIXOS) contains 160 AGN compiled from serendipitous sources detected in pointed observations made with *ROSAT*. The optical data was obtained using the Isaac Newton (INT) and William Herschel Telescopes (WHT) at La Palma. As well as continuum luminosities and spectral slopes, the data contains EW, and FWHM for several optical emission lines. Because of the range in redshift of the objects (0.03–2.92 with most objects at $z < 1.0$) it is clearly not possible to measure these quantities for all the emission lines with only the WHT and INT. Thus when considering the sample of AGN in one particular line the sample size of 160 is greatly reduced and in some cases becomes too small to be of any real use. We will therefore concentrate on MgII with a sample size of 113. Fig. 1 shows the luminosity distribution for this sample.

We note that the X-ray luminosities given in Puchnarewicz et al. (1997) are not corrected for absorption intrinsic to the source AGN. However from figure 17 of Puchnarewicz et al. (1996) we see that 62% of systems have an absorbing column, N_{H}, of less than $10^{21}\,\mathrm{cm^{-2}}$ rising to

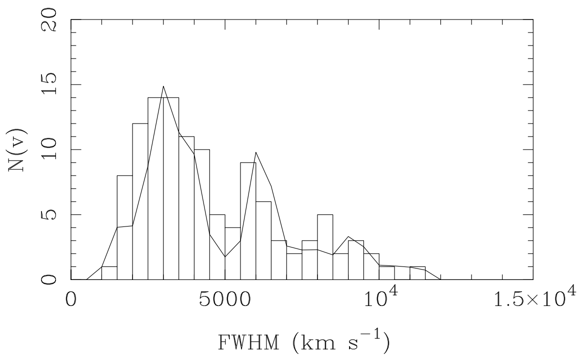

Figure 2. Linewidth distribution curves and data histograms for MgII.

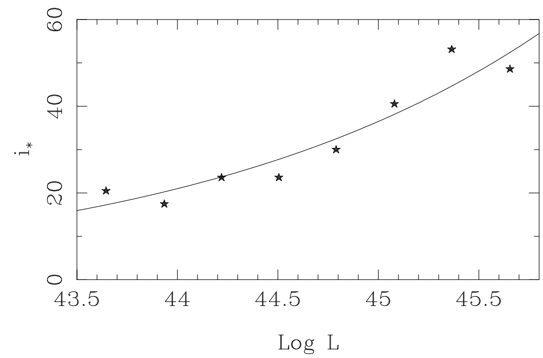

Figure 5. Relation between i_* and $\log L$ found by taking average luminosity and calculated $\sin i_*$ in each luminosity bin. The curve is $i_* = 21.0L_{44}^{0.24}$.

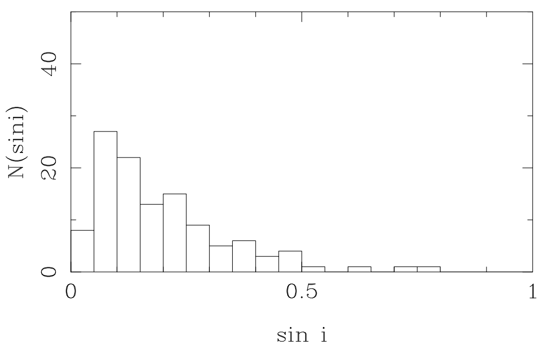

Figure 3. $\sin i$ distribution for MgII calculated using the values of a, b and α as in fig. 2.

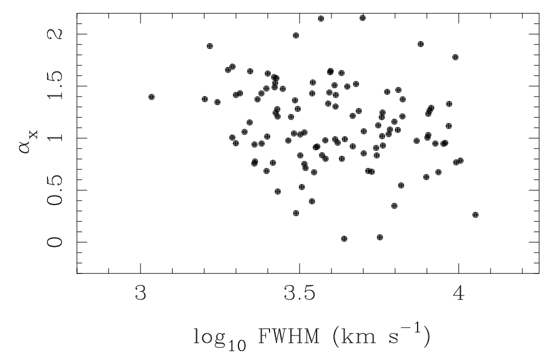

Figure 6. Observed α_X vs FWHM$_{\rm MgII}$. Note the weak anti-correlation between these two properties.

85% at $N_{\rm H} < 1.5 \times 10^{21}$ cm^{-2}. At $N_{\rm H} = 1.5 \times 10^{21}$ cm^{-2} for a standard power law spectrum we find that the source luminosity should be $\sim 30\%$ higher than observed. For the values of a, b and α used here this gives values of i that are $\sim 10\%$ higher. In most sources the effect will be much less than this and is therefore neglected.

5 RESULTS

Using (4) and iterating to a solution for $T(\sin i, L)$ we can predict the linewidth distribution for MgII. We obtain the values $a = 1000 {\rm km\,s^{-1}}$, $b = 25000 {\rm km\,s^{-1}}$ and $\alpha = -0.2$. This value for α is well constrained by consideration of both the Baldwin effect for MgII and the observed correlation between FWHM and line equivalent width (Rudge & Raine 1998). The parameters a and b are then constrained tightly as b gives the spread of the distribution and a its centroid position. Further constraints are placed on a and b by the obvious requirement that $0 < \sin i < 1$. Fig. 2 shows a histogram of the data overlaid with the predicted distribution curve.

Fig. 3 shows the self-consistent distribution of $\sin i$ calculated from (3). Since there are no strong angle-dependent selection effects, this distribution is at first sight incompatible with our interpretation of i. However, fig. 4 shows how the distribution of $\sin i$ changes with luminosity, the division being into eight equally sized bins on a logarithmic scale between $\log L = 43.5$ and $\log L = 45.8$.

It is clear that the maximum value of $\sin i$, and therefore i_* increases with luminosity. Within each bin the $\sin i$ distribution is more uniform over the range $i < i_*$ than for the sample as a whole. From the dependence of i_* upon L shown in fig. 4 we fit a relation of the form

$$i_* = 21.0L_{44}^{0.24} \text{ degrees} \qquad (5)$$

Finally table 5 shows the sources used, their luminosities, linewidths and the calculated inclination angle.

6 RELATION BETWEEN FWHM AND α_X

Several samples of AGN have shown an anti-correlation between FWHM and α_x (Borson & Green 1992; Wandel & Boller 1998; Puchnarewicz et al. 1997) particularly for FWHM$_{\rm H\beta}$. The viewing angle dependence of the FWHM leads us to expect that α_X might depend on i also.

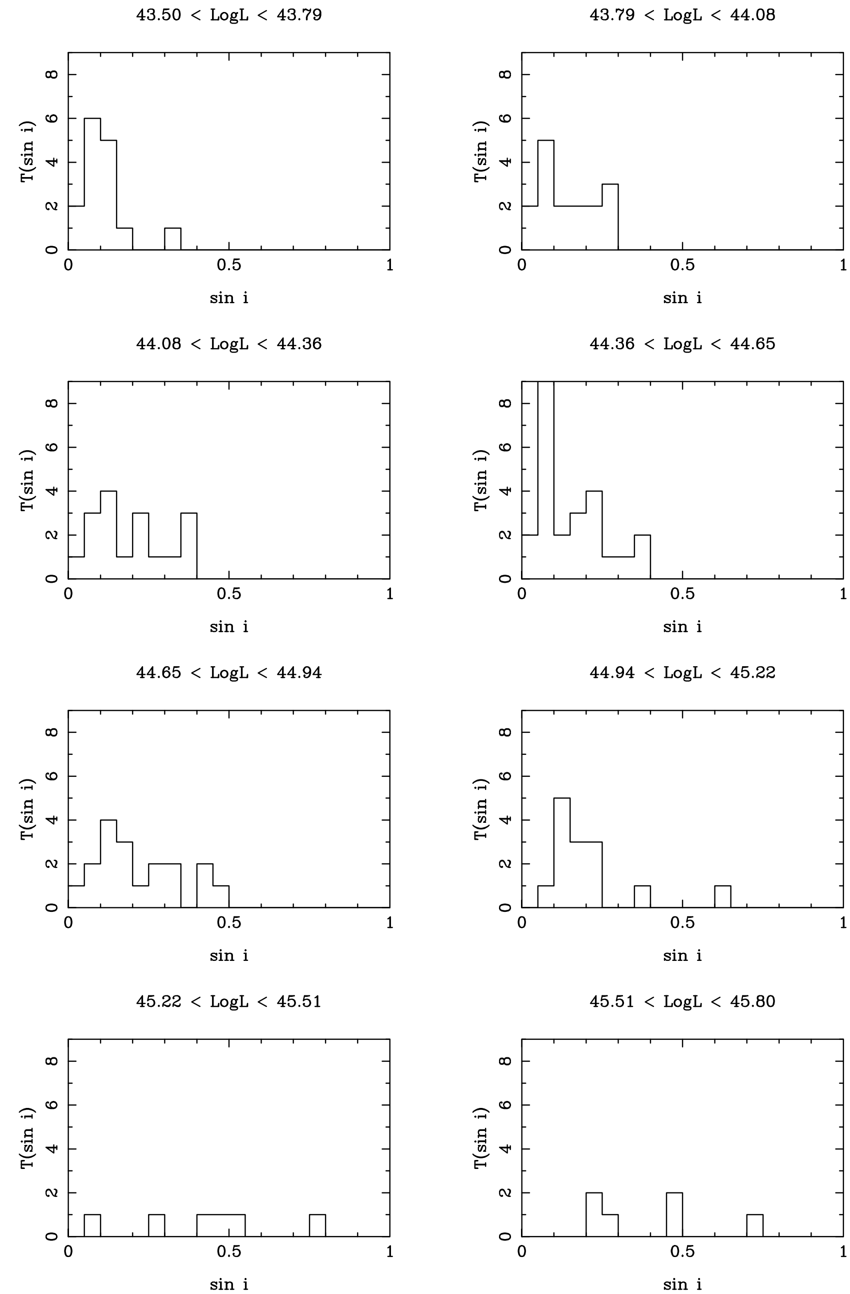

Figure 4. Change in distribution of $\sin i$ with luminosity for MgII.

Puchnarewicz et al. (1997) also suggest that there is absorption of the soft X-rays in the objects with broader lines, i.e. the more edge-on objects. This might indicate a model in which the soft X-rays are increasingly absorbed by some sort of torus of dust/gas as the observer moves to a larger viewing angle. In the sample used here there is in fact a weak correlation between $\alpha_{\rm X}$ and $\rm FWHM_{MgII}$ (fig. 6).

We consider whether this correlation is at least in part due to the relation between i_* and L. Fig. 7 shows $\alpha_{\rm X}$ plotted against $\sin i$ in luminosity bins. Notice that their is no obvious anti-correlation between $\sin i$ and $\alpha_{\rm X}$ with the data divided in this way. In fact some luminosity bins indicate the opposite is true. This suggests that viewing angle is not the primary parameter determining $\alpha_{\rm X}$.

7 DISCUSSION

In this paper we have provided further evidence that the BLR in AGN is axisymmetric. The case for axisymmetry in radio-loud systems has always been strong with the observed correlations between line width, R and $\alpha_{\rm ox}$. With no such obvious measure of inclination angle for radio-quiet systems the case is much harder to argue. The RIXOS data used here is made up of both radio-loud and quiet systems. There is

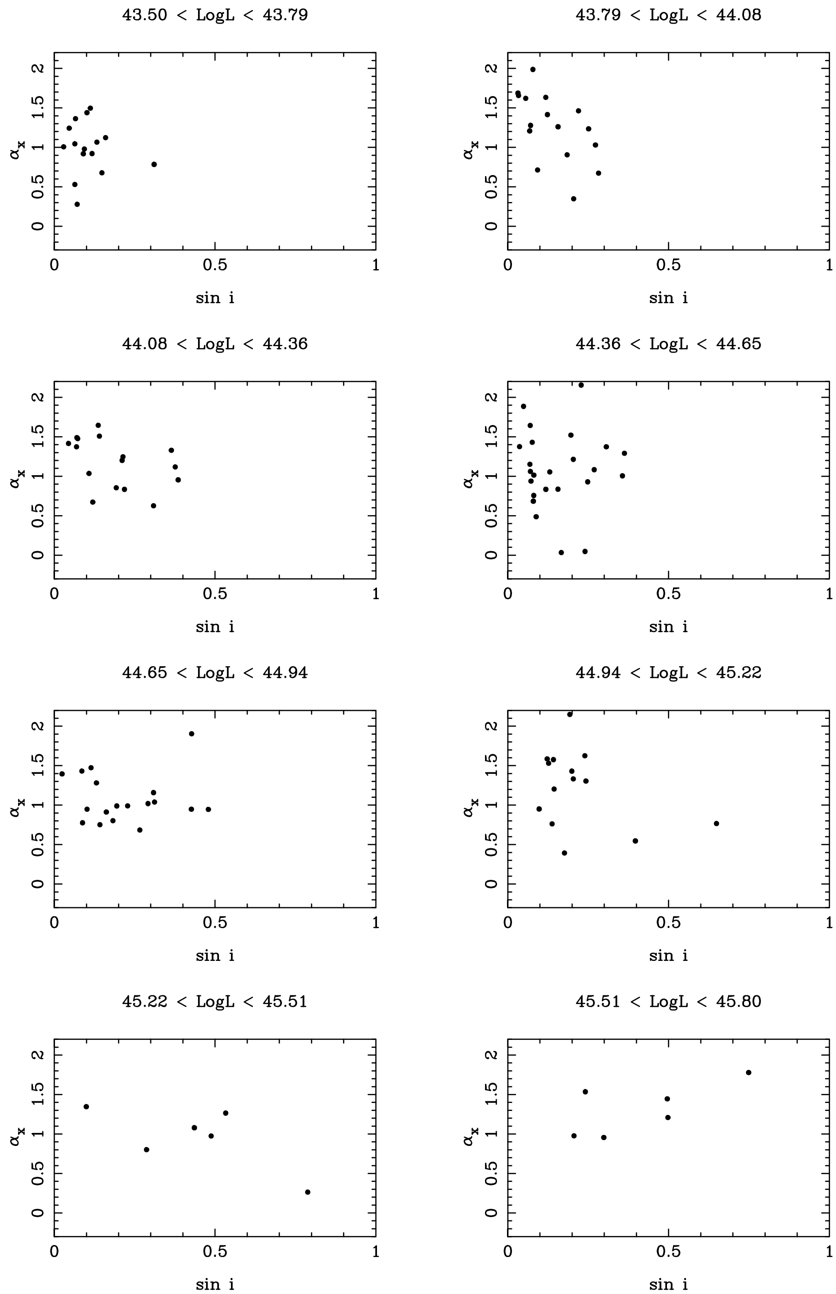

Figure 7. Observed α_X vs calculated $\sin i$ for the objects with measured MgII divided into luminosity bins. There is no obvious correlation, in either sense, common to all luminosity bins.

no obvious failing of an axisymmetric model when applied to all systems, as would be expected if the radio-quiets were not axisymmetric. Also, with no clear difference between the distribution of linewidths for radio-loud and radio-quiet systems, it is reasonable to expect that the linewidths in radio-quiet systems are, as in radio-loud systems, viewing angle dependent.

Marziani et al. (1996) argue the case for a significant difference between the structure of the BLR in radio-loud and radio-quiets systems. They show that the Hβ line profiles are predominantly redshifted and asymmetric in radio-louds whilst being usually unshifted and symmetric in the radio-quiets. Conversely CIV is largely unshifted and symmetric in radio-louds and blueshifted and asymmetric in radio-quiets. However, further inspection of the distribution of these properties shows that they are consistent with a single model for the BLR when we take into account the effect of luminosity on opening angle. In the context of a disc-wind model such as those of Cassidy & Raine (1996) and Chiang & Murray (1996) we would expect the lines to be blue shifted if the viewing angle is along (or close to) the disc. This effect will be stronger in CIV than in Hβ which tends to be produced close to the disc where the outward velocity component is smaller and the outer clouds obscure the emission. This ob-

Table 1. Sample data for the RIXOS objects with measured $\mathrm{FWHM_{MgII}}$. Note: Field ID (1), Source number (2) and linewidths (5) are taken from Puchnarewicz et al. 1997; α_{x} (3) is from Puchnarewicz et al. 1996; $\log L$ for the ROSAT 0.5–2 keV band is from E.M. Puchnarewicz (private communication) and $\sin i$ (6) is as calculated by the method outlined in this paper.

FID (1)	Snum (2)	α_{x} (3)	$\log L$ (4)	$\mathrm{FWHM_{MgII}}$ (5)	$\sin i$ (6)
110	1	1.687	43.816	1945.5	0.031
110	8	1.005	44.473	7974.5	0.356
110	34	0.033	44.363	4366.6	0.166
110	50	0.989	44.779	4088.5	0.194
122	14	1.621	43.893	2511.7	0.055
123	41	0.763	45.159	2606.3	0.137
123	42	1.045	43.664	3035.8	0.064
123	46	0.047	44.464	5654.4	0.240
123	66	1.030	43.943	8022.6	0.272
123	85	1.885	44.644	1651.0	0.048
125	14	0.956	45.540	4164.4	0.298
125	17	1.477	44.271	2486.1	0.072
133	22	0.802	45.398	4293.5	0.286
205	11	1.430	44.411	2398.3	0.075
205	12	1.430	45.185	3463.3	0.199
205	22	1.645	44.237	3958.3	0.136
205	34	1.201	44.198	5729.7	0.211
206	6	0.672	44.279	3510.4	0.119
206	9	0.487	44.371	2700.0	0.088
206	507	0.979	43.712	3808.7	0.093
206	522	1.373	44.338	2331.7	0.068
208	2	1.278	44.059	2690.0	0.070
208	55	0.767	45.221	9816.8	0.649
211	30	0.951	45.182	1993.3	0.097
211	35	1.123	43.754	5584.9	0.159
212	6	0.836	44.597	3719.0	0.155
212	16	0.954	44.345	9069.2	0.385
212	25	1.373	44.567	6667.0	0.306
213	7	0.713	44.007	3300.6	0.092
213	11	−0.49	44.309	7363.2	0.299
213	17	1.415	43.984	4107.5	0.123
213	19	1.415	44.117	1994.3	0.044
213	20	1.015	44.410	2501.2	0.080
215	1	0.977	45.621	2914.0	0.205
215	19	1.375	44.396	1592.6	0.036
215	32	1.208	44.001	2696.4	0.067
216	7	0.834	44.337	5526.4	0.218
217	3	1.214	44.590	4641.9	0.203
217	21	1.261	44.023	4852.8	0.156
217	34	1.332	44.976	3888.3	0.203
217	35	0.921	43.640	4646.8	0.117
217	59	1.117	44.243	9304.6	0.376
218	1	0.854	44.318	5028.3	0.192
218	9	1.508	44.222	4071.8	0.140
218	27	1.055	44.571	3273.2	0.130
219	15	1.586	44.944	2629.2	0.122
219	45	0.546	45.096	6590.6	0.396
219	48	0.946	44.806	8955.0	0.479
220	13	0.919	43.785	3593.6	0.090
220	18	0.784	43.685	10127.	0.310
221	2	0.939	44.445	2281.8	0.072
221	35	0.948	44.845	2401.9	0.101
224	201	1.265	45.238	8099.2	0.532
226	41	1.079	45.333	6435.1	0.435
226	114	0.756	44.605	2279.0	0.080
227	19	1.346	45.504	1744.9	0.099
227	37	1.209	45.528	6654.0	0.497
227	513	0.912	44.761	3553.8	0.161

Table 1 – *continued* Data for objects in RIXOS sample with measured $\mathrm{FWHM_{MgII}}$.

FID (1)	Snum (2)	α_{x} (3)	$\log L$ (4)	$\mathrm{FWHM_{MgII}}$ (5)	$\sin i$ (6)
228	1	0.263	45.317	11289.	0.788
234	1	1.445	45.760	5957.9	0.495
234	33	1.904	44.933	7597.9	0.427
236	5	1.363	43.691	3058.9	0.066
236	21	1.474	44.697	2799.2	0.114
240	15	1.431	44.923	2054.1	0.085
240	82	0.673	43.848	8635.6	0.282
245	4	1.329	44.172	9330.3	0.363
252	9	1.246	44.207	5762.9	0.213
252	34	0.906	44.042	5500.9	0.184
252	36	1.039	44.821	6023.7	0.311
253	5	1.158	44.712	6279.0	0.308
254	10	1.576	45.152	2672.3	0.141
254	11	1.304	45.184	4100.3	0.242
254	41	1.234	43.789	8023.5	0.251
255	13	1.634	44.002	3943.3	0.117
255	19	2.155	44.640	4988.5	0.227
257	14	0.776	44.722	2289.8	0.087
257	20	1.019	44.795	5742.9	0.291
257	38	0.990	44.919	4387.0	0.227
258	5	1.643	44.469	2210.5	0.069
258	30	1.066	43.665	5031.0	0.132
259	5	0.948	44.700	8445.0	0.426
259	7	0.530	43.538	3213.5	0.063
259	11	0.929	44.482	5777.5	0.248
260	8	0.974	45.263	7374.4	0.487
260	44	0.393	44.969	3458.0	0.176
262	1	1.520	44.469	4756.4	0.196
262	34	1.439	43.777	3921.5	0.101
265	17	1.006	43.741	1942.8	0.028
268	11	0.626	44.211	7908.2	0.308
271	2	1.987	43.909	3078.8	0.078
271	7	1.626	45.065	4282.0	0.239
272	8	1.535	45.526	3480.2	0.241
272	18	1.083	44.517	6079.5	0.268
272	28	1.463	44.010	6463.0	0.219
273	4	1.530	44.986	2648.9	0.126
273	18	1.496	43.650	4464.5	0.111
273	22	2.149	44.988	3691.0	0.192
273	23	1.243	43.549	2658.8	0.046
278	9	0.802	44.816	3814.6	0.182
281	21	0.677	43.726	5329.8	0.147
283	6	0.685	44.840	5194.1	0.265
283	21	0.349	43.945	6278.3	0.204
286	2	1.778	45.527	9763.7	0.748
293	1	0.834	44.476	3177.5	0.118
293	12	0.684	44.392	2488.9	0.079
294	1	1.291	44.446	8196.2	0.362
302	14	1.151	44.451	2202.9	0.068
302	18	0.752	44.713	3272.7	0.141
305	18	0.279	43.776	3081.2	0.071
305	34	1.060	44.566	2122.8	0.070
110	35	1.656	43.944	1884.0	0.033
122	1	1.396	44.852	1083.0	0.024
208	18	1.489	44.096	2639.2	0.070
216	33	1.035	44.329	3176.6	0.107
262	12	1.281	44.685	3120.1	0.131
293	10	1.204	44.948	2972.2	0.143

scuration may also cause us to see Hβ predominantly from the far side of the disc giving a tendency towards redshifted lines when the opening angle is large. In general radio-loud sources are observed at higher luminosities than radio-quiets and thus have a larger range of possible viewing angles to the BLR. Thus we would expect to see a blueshifted CIV line in a smaller percentage of sources for radio-louds than radio-quiets. The effect is increased by the fact that in lower luminosity radio-quiets the opening angle is small and the radial velocity component is significant at all viewing angles. Thus, rather than showing that the radio-loud and radio-quiets have different BLR structures, figure 4 of Marziani et al. (1996) can be interpreted as the change in the range of those properties observed due to the effect of increasing opening angle with luminosity.

We have shown that for the RIXOS sample (Puchnarewicz et al. 1996; Puchnarewicz et al. 1997) our calculation of the value of $\sin i$ for each system gives a realistic distribution of angles. This distribution is, however, not uniform as originally assumed (Rudge & Raine 1998). When only a small range of luminosity is considered, it does become more uniform, but has a luminosity dependent maximum value for $\sin i$. This result further supports the assertion that the BLR is axisymmetric. In unified models it is expected that the BLR, whether axisymmetric or not, can be viewed only up to some maximum inclination, i_*, before being obscured. It is also natural to expect that i_* will be dependent upon luminosity in the sense that higher luminosity systems will have larger opening angles than low luminosity sources. In an axisymmetric BLR model we have confirmed this result. Providing evidence for this change in opening angle with luminosity has important implications for unified models. Previously, the opening angle, at least for radio-quiet AGN, has been estimated from the observed ratio of Seyfert 1s to Seyfert 2s. Our results show that this estimate needs to be carried out at each luminosity rather than for complete samples.

We have also been able to show that the spectral index, α_X, is not dependent primarily upon viewing angle. It is not unreasonable to expect that the soft X-rays are obscured in more edge-on systems giving a harder continuum. This was in fact predicted from the RIXOS data by Puchnarewicz et al. (1997). Such a viewing angle dependence would also explain the observed correlation between $\mathrm{FWHM}_{\mathrm{H}\beta}$ and spectral index observed in other samples e.g. Boroson & Green (1992), where the broader lines correspond to the harder X-ray spectrum. However, fig. 7 shows that when we plot α_X against $\sin i$ in luminosity bins we do not see the expected anti-correlation between α_X and $\sin i$. In fact at some luminosities the data suggests that a positive correlation is more likely. It appears that the observed anti-correlation is driven at least partly by the dependence of $\sin i_*$ upon L, and is not a consequence of an orientation dependent observed X-ray spectrum.

8 CONCLUSIONS

We have shown that if the kinematics of MgII emission is axisymmetric then the cone opening angle in the unified model is dependent upon luminosity. The self-consistency of the picture provides support for the view that the BLR is axisymmetric. As a consequence we deduce that the X-ray spectral index is not primarily dependent upon viewing angle.

9 ACKNOWLEDGEMENTS

CMR acknowledges the support of PPARC, in the form of a research studentship.

REFERENCES

Antonucci R., 1993, ARA&A, 31 ,473
Boroson T.A., 1992, ApJ, 399, L15
Boroson T.A., Green R.F., 1992, ApJS, 80, 109
Boyle B.J., Shanks T., Peterson B.A., 1988, MNRAS, 235, 935
Boyle B.J., Griffiths R.E., Shanks T., Stewart G.C., Georgantopoulos I., 1993, MNRAS, 260, 49
Boyle B.J., Shanks T., Georgantopoulos I., Stewart G.C., Griffiths R.E., 1994, MNRAS, 271, 639
Brotherton M.S., 1996, ApJS, 102, 1
Cassidy I., Raine D.J., 1996, A&A, 310, 49
Chiang J., Murray N., 1996, ApJ, 466, 704
Corbin M.R., 1997, ApJS, 113, 245
Dumont A-M., Collin–Souffrin S., 1990, A&A, 229, 313
Gaskell C.M., 1982, ApJ, 263, 79
Goad M.R., Koratkar A.P., Axon D.J., Korista K.T., O'Brien P.T., 1999, ApJL, 512, 95
Korista K. et al., 1995, ApJS, 97,285
Marziani P., Sulentic J.W., Dultzin–Hacyan D., Calvani M., Moles M., 1996, ApJS, 104, 37
Pei Y.C., 1995 ApJ, 438, 623
Puchnarewicz E.M., Mason K.O., Romero–Colmenero E., Carrera F.J., Hasinger G., McMahon R.G., Mittaz J.P.D., Page M.J., Carballo R., 1996, MNRAS, 281, 1243
Puchnarewicz E.M., Mason K.O., Carrera F.J. Brandt W.N., Cabrera–Guera F., Carballo R., Hasinger G., McMahon R., Mittaz J.P.D., Page M.J., Perez–Fouron I., Schwope A., 1997, MNRAS, 291, 177
Robinson A., 1995, MNRAS, 272, 647
Rudge C.M., Raine D.J., 1998, MNRAS, 297, L1
Rudge C.M., Raine D.J., 1999, accepted for publication in MNRAS
Stirpe G.M., 1991, Astron. Astrophys., 247, 3
Wandel A., Boller Th., 1998, A&A, 331, 884
Wanders J., Horne K., A&A, 1994, 289, 76
Wills B.J., Browne I.W.A., 1986, ApJ, 302, 56
Wills B.J., Brotherton M.S., Fang D., Steidel C.C., Sargent W.L.W., 1993, ApJ, 415, 563
Wills B.J., Brotherton M.S., 1995, ApJ, 448, L81